Interfering Tunneling Paths through Magnetic Molecules on Superconductors: Asymmetries of Kondo and Yu-Shiba-Rusinov Resonances

Laëtitia Farinacci,[1] Gelavizh Ahmadi,[1] Michael Ruby,[1] Gaël Reecht,[1] Benjamin W. Heinrich,[1] Constantin Czekelius,[2] Felix von Oppen,[3] and Katharina J. Franke[1]

[1]*Fachbereich Physik, Freie Universität Berlin, Arnimallee 14, 14195 Berlin, Germany*

[2]*Institut für Organische Chemie und Makromolekulare Chemie, Heinrich-Heine-Universität Düsseldorf, Universitätsstrasse 1, 40225Düsseldorf, Germany*

[3]*Dahlem Center for Complex Quantum Systems and Fachbereich Physik, Freie Universität Berlin, Arnimallee 14, 14195 Berlin, Germany*

(Received 10 July 2020; revised 10 October 2020; accepted 19 November 2020; published 18 December 2020)

Magnetic adsorbates on superconductors induce a Kondo resonance outside and Yu-Shiba-Rusinov (YSR) bound states inside the superconducting energy gap. When probed by scanning tunneling spectroscopy, the associated differential-conductance spectra frequently exhibit characteristic bias-voltage asymmetries. Here, we observe correlated variations of Kondo and YSR asymmetries across an Fe-porphyrin molecule adsorbed on Pb(111). We show that both asymmetries originate in interfering tunneling paths via a spin-carrying orbital and the highest occupied molecular orbital (HOMO). Strong evidence for this model comes from nodal planes of the HOMO, where tunneling reveals symmetric Kondo and YSR resonances. Our results establish an important mechanism for the asymmetries of Kondo and YSR line shapes.

DOI: 10.1103/PhysRevLett.125.256805

Exchange coupling a magnetic adsorbate to a metallic substrate induces a many-body Kondo resonance at the Fermi level. Already initial observations of the Kondo effect of single magnetic adatoms by scanning tunneling spectroscopy revealed asymmetric Fano line shapes [1,2]. These have been interpreted as arising from interference between tunneling via the adatom and direct tunneling into the continuum of electronic states of the metallic substrate [3–6]. On superconducting substrates, the exchange coupling also binds a pair of Yu-Shiba-Rusinov (YSR) states inside the superconducting energy gap [7–9], which coexist with the Kondo resonance outside of the gap [10–12]. Corresponding tunneling-spectroscopy resonances appear for both bias polarities with identical energies but asymmetric strengths [13–15]. This asymmetry is commonly associated with differences between the electron and hole components of the YSR wave function due to breaking of particle-hole symmetry by additional potential scattering [7–9,16–18].

Within these conventional interpretations, the asymmetries of the Kondo and YSR resonances seem unrelated. Surprisingly, our measurements reveal striking correlations between these asymmetries when tracking them as a function of tip position above a Fe-5,10,15,20-tetra-pyridyl-porphyrin molecule (FeTPyP) with its spin moment derived from the Fe center and large extent over the organic ligand [19–21]. Placing the molecules on a Pb(111) substrate, we investigate the YSR states in the presence of superconductivity and the Kondo resonance while quenching superconductivity by a magnetic field. This allows us to record YSR and Kondo spectra with the same tip across the very same molecule.

These correlations suggest that the origins of the Kondo and YSR asymmetries have to be reconsidered for our system. Recent theoretical work by Frank and Jacob suggested that the Kondo asymmetry of magnetic adatoms originates from a parallel tunneling path through s or p orbitals within the atom itself [22] (see also [23]). While their predictions have not yet been validated by experiment, experiments investigated spatial variations of the Fano line shape in (metal-organic) molecules [24–28]. YSR states were observed in several molecular systems, though without the aim of spatially resolving their asymmetries [15,30–36]. We find that parallel tunneling through two molecular orbitals naturally explains the correlations between the Kondo and YSR resonances, consistent with and extending the basic picture proposed in Ref. [22].

FeTPyP-Cl molecules were evaporated from a Knudsen cell heated to 400°C onto a Pb(111) surface held at 40°C. This leads to the formation of densely-packed islands, with scanning-tunneling-microscope (STM) images of the molecules displaying a bright elongated shape [Fig. 1(a)]; for details, see Supplemental Material (SM) [37]. This appearance is attributed to a saddle-shaped conformation with two upward- and two downward-tilting pyrrole groups, reflecting competition between molecule-substrate interactions and intramolecular steric hindrance [19–21,38,39]. The absence of a central protrusion shows that the central Cl

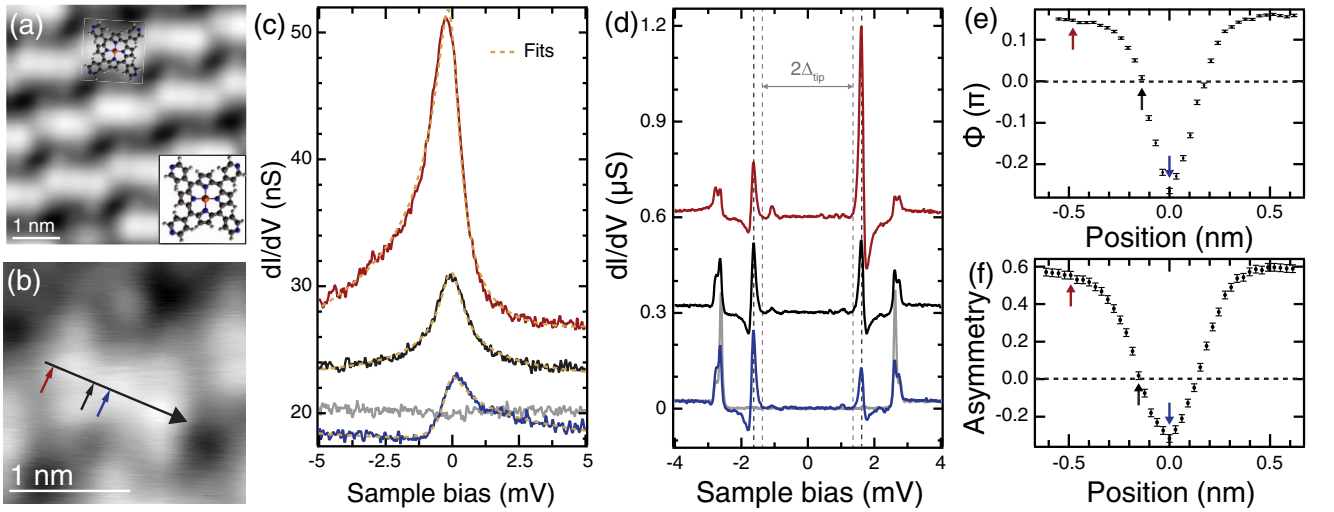

FIG. 1. (a) Topography of molecular island ($V = -800$ mV, $I = 50$ pA). Inset: molecular structure of the FeTPyP molecule. (b) Closeup of one molecule with the color-coded locations of the spectra in (c),(d) marked by arrows ($V = 5$ mV, $I = 100$ pA). (c) dI/dV spectra of the Kondo resonance, measured in a magnetic field of $B = 1.5$ T. Gray spectrum taken on the bare Pb(111) substrate, colored spectra taken at locations marked in (b) (feedback opened at $V = 5$ mV, $I = 100$ pA, lock-in $V_{\mathrm{rms}} = 100$ μeV). Spectra are offset for clarity. Fits of the resonances to the Frota-Fano function [Eq. (1)] are shown as dashed brown lines. (d) dI/dV spectra recorded with superconducting tip and substrate in the absence of the B field. The YSR states (marked by dashed black lines) appear as a pair of resonances symmetric in energy, but asymmetric in intensity. The tip gap is indicated by gray dashed lines. Peaks below this energy are due to thermal excitations of the YSR states. Gray spectrum exhibiting BCS coherence peaks taken on the bare substrate, colored spectra taken at locations marked in (b). Spectra are offset for clarity (feedback opened at $V = 5$ mV, $I = 100$ pA, lock-in $V_{\mathrm{rms}} = 15$ μeV). (e) Asymmetry parameter ϕ deduced from a Frota-Fano fit of the Kondo spectra along the line indicated in (b) (zero marking the molecule's center). Error bars represent the fit error. (f) Asymmetry $(H_+ - H_-)/(H_+ + H_-)$ of the YSR resonances along the line indicated in (b). Peak heights $H_\pm$ are determined by a search algorithm for local maxima, estimated error of 0.02 due to noise.

ligand detaches from all molecules during adsorption [21]. This dechlorination reduces the Fe oxidation state from +3 to +2, and the molecule is expected to lie on the surface in an integer spin state [19–21,40]. STM images reveal two distinct types of molecules. Here, we focus on the majority type [Fig. 1(a)], which exhibits both Kondo and YSR resonances. Spectra taken on the other type (not shown) exhibit inelastic spin excitations reflecting different interaction strengths with the substrate.

To probe the Kondo resonance and its spatial variation along the FeTPyP molecule, we record dI/dV spectra at $T = 1.1$ K in a magnetic field of 1.5 T which quenches superconductivity in both substrate and tip. We find a strong resonance with a shoulder at negative bias voltages on the upper pyrrole [Figs. 1(b) and 1(c), red line]. As the tip position moves toward the center of the molecule, the peak height reduces and eventually inverts its bias asymmetry at the Fe center [Figs. 1(b) and 1(c), blue line]. These resonances are well fitted by Fano-Frota line shapes [41,42]

$$\frac{dI}{dV} = A\mathrm{Re}\left(e^{i\phi}\sqrt{\frac{i\Gamma/2}{eV-\omega_0+i\Gamma/2}}\right) + B, \qquad (1)$$

where A is the amplitude of the resonance at energy ω_0, Γ a width parameter, ϕ a phase characterizing the asymmetry, and B a bias-independent background. We find the same width of (0.77 ± 0.03) meV for all spectra along the molecule, while the asymmetry ϕ varies continuously and eventually inverts [Fig. 1(e)]. [Fits are shown as dashed lines in Fig. 1(c); for a complete set of spectra along the line indicated in Fig. 1(b), see SM [37].] The narrow line shapes and characteristic asymmetries suggest that these are Kondo resonances probed by interfering tunneling paths [22,43–45]. An observed splitting of the resonance at larger magnetic fields further confirms the magnetic origin (see SM [37]).

In addition to the Kondo resonance for a normal-state substrate, the exchange coupling also induces YSR bound states for a superconducting substrate. We investigate their dependence on tip position in the absence of the external magnetic field. Then, the Pb tip is also superconducting, increasing our energy resolution beyond the Fermi-Dirac temperature limit and shifting all features in the dI/dV spectra by the tip's energy gap $\Delta = 1.35$ mV [46]. A spectrum taken on the bare Pb(111) substrate is shown in gray in Fig. 1(c). The superconducting energy gap is flanked by two pairs of coherence peaks at ± 2.65 mV and ± 2.8 mV, reflecting the two-band character of superconductivity in Pb [46].

dI/dV spectra on the FeTPyP molecule show a pair of YSR resonances at ± 1.6 mV inside the superconducting

energy gap. Consistent with the observation of a constant Kondo width, their energies are independent of tip position above the molecule, indicating that the exchange coupling between substrate and molecule induces a single pair of YSR states. Unlike the energy, the heights $H_{\pm}$ of the YSR resonances are different at positive and negative bias voltages. In Fig. 1(f), we plot the measured asymmetry $(H_+ - H_-)/(H_+ + H_-)$ vs tip position. Comparison with the asymmetry variations of the Kondo resonance in Fig. 1(g) reveals striking similarities. In particular, we observe a particle-hole symmetric YSR spectrum exactly where the Kondo peak exhibits a symmetric Frota peak [black spectra in Figs. 1(c) and 1(d)]. Comparing spectra on both sides of this symmetry point, we observe an inversion of the asymmetry of the YSR states, which parallels the asymmetry inversion of the Kondo resonance.

To further corroborate these correlations, we map out the Kondo and YSR resonances across the entire molecule. Figure 2(a) presents an STM image (gray scale) of a single FeTPyP molecule superimposed with zero-bias dI/dV intensities extracted from a densely spaced grid of dI/dV spectra. The four-lobe structure shows that the Kondo intensity is largest on the molecular ligand. We extract the local amplitude A [Fig. 2(b)] and phase parameter ϕ [Fig. 2(c)] of the Kondo resonance across the entire molecule by fitting all dI/dV spectra to the Fano-Frota line shape [Eq. (1)]. The amplitude naturally follows the dI/dV intensity at zero bias. Consistent with the line profile in Fig. 1(e), the asymmetry exhibits reversed signs above Fe atom and ligand.

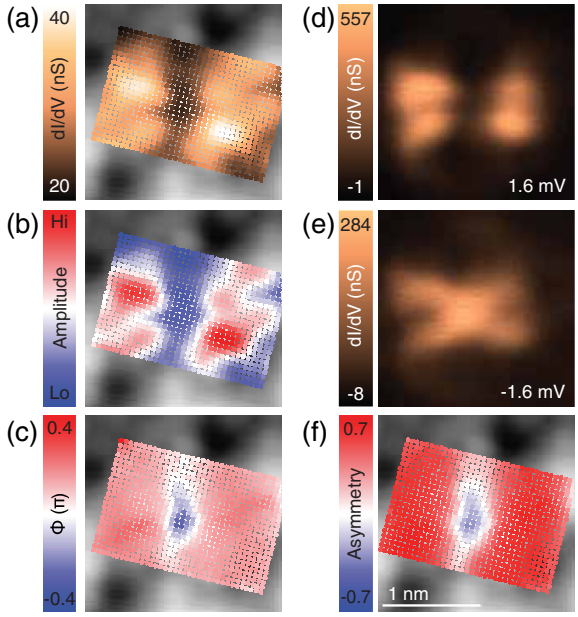

FIG. 2. (a)–(c) Topography of the molecule (background black-white images, $V = 5$ mV, $I = 100$ pA) with superimposed color plots extracted from a grid of spectra (feedback opened at $V = 5$ mV, $I = 100$ pA, signal modulated with $V_{\mathrm{rms}} = 100$ μeV). Color plots show (a) the dI/dV signal at $V = 0$ mV, (b) the amplitude A, and (c) the asymmetry parameter ϕ extracted from the Fano-Frota fits of the Kondo resonance to Eq. (1). (d) dI/dV map of the YSR state recorded along the topography contour of Fig. 1(b) ($V = 5$ mV, $I = 100$ pA) at positive bias voltage $V = 1.6$ mV and (e) at negative bias voltage $V = -1.6$ mV ($V_{\mathrm{rms}} = 15$ μeV). (f) Asymmetry of the YSR state extracted from a grid of spectra taken (feedback opened at $V = 5$ mV, $I = 100$ pA, signal modulated with $V_{\mathrm{rms}} = 15$ μeV). Background black-white topography images are the same image as in Fig. 1(b). All images are recorded above the same area.

The YSR intensities at positive and negative bias voltages are shown in Figs. 2(d) and 2(e). At positive bias voltage, the YSR intensity has its maxima on the ligand, resembling the map of the amplitude of the Kondo resonance. At negative bias voltage, the YSR intensity is largest at the Fe center. These intensity distributions are reflected in the map of the asymmetry shown in Fig. 2(f). In agreement with the line profile in Fig. 1(f), we find reversed asymmetries at the Fe center and the ligand. This map of the YSR asymmetry is remarkably similar to the map of the Kondo asymmetry in Fig. 2(c). These experimental observations strongly suggest a common origin of the Kondo and YSR asymmetries.

The observations of a constant Kondo-resonance width and YSR energy indicate that tunneling probes the same excitations across the entire molecule. While details of the spin state are not central to our model, the magnetic-field splitting of the Kondo resonance suggests an $S = 1$ impurity spin, carried by hybrid orbitals of the ligand-field-split d states and the organic ligand [20] (see also SM [37]). The exchange coupling of one of the spin-carrying orbitals leads to the Kondo resonance [47] and the pair of YSR states, both of which can be probed with varying intensity across the entire molecule.

While virtual excitations of this orbital generate both exchange and potential scattering of substrate electrons (as described by a Schrieffer-Wolff transformation), the pronounced Kondo correlations imply that exchange coupling is strongly dominant at low energies. Without additional tunneling channels, one thus expects not only a symmetric Kondo line shape, but also symmetric YSR resonances, reflecting approximately equal electron and hole YSR wave functions.

The asymmetries of the Kondo and YSR resonances point to a second tunneling path which exists in parallel to tunneling via this strongly exchange-coupled orbital. dI/dV spectra taken over a larger voltage range [Fig. 3(a)] reveal one (or several) resonances beginning at -360 mV which we refer to as the highest occupied molecular orbital (HOMO) and which extends toward the Fermi level. We associate the second tunneling path with this orbital. A constant density-of-states map shows large intensity at the Fe center, separated by two nodal planes from maxima at the upper pyrroles of the molecular saddle

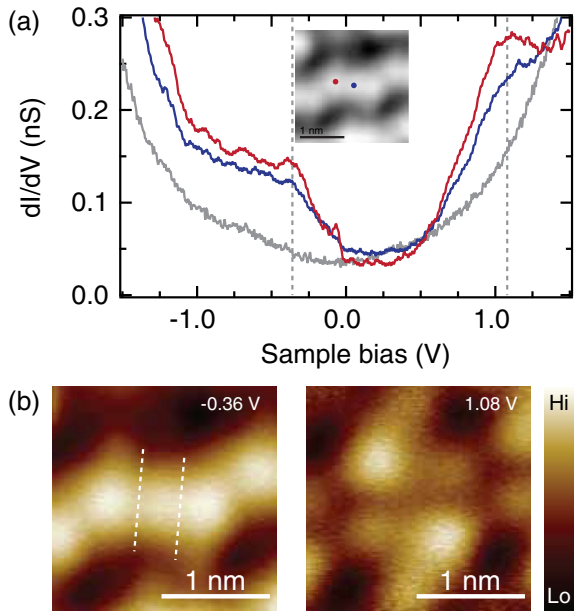

FIG. 3. (a) dI/dV spectra taken on FeTPyP molecule (color-coded locations marked in inset) and on the bare Pb substrate (gray) (feedback opened at $V = 2$ V, $I = 500$ pA, and signal modulated with $V_{\mathrm{rms}} = 10$ mV). Dashed lines indicate locations of resonances identified as HOMO ($V \simeq -360$ mV) and LUMO ($V \simeq 1.08$ V). (b) Iso-density-of-states maps of one FeTPyP molecule recorded at bias voltages as indicated in the top-right corners and corresponding to HOMO (left) and LUMO (right) resonances (signal modulated with $V_{\mathrm{rms}} = 2$ mV and regulated at a conductance of 2.06 nS). Nodal planes are indicated by dashed lines.

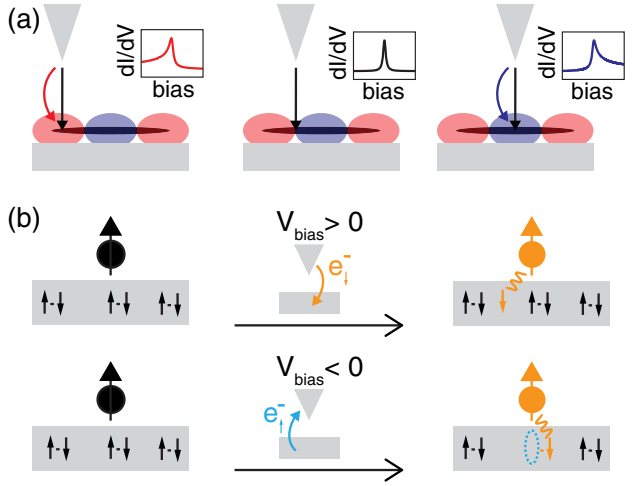

FIG. 4. (a) Schematic HOMO wave function (red and blue) and spin-carrying molecular orbital (gray) on a surface for different tip positions, with the corresponding Kondo line shapes in the insets. At the HOMO nodal plane, the line shape is symmetric. (b) Tunneling into the superconducting substrate at positive (top) and negative bias (bottom) populating the YSR excitation (right) from an unscreened-spin ground state (left). Because of spin polarization of the YSR state and singlet Cooper pairing, the spin of electrons tunneling (into) from the substrate is (anti)parallel to the impurity spin.

[Fig. 3(b)]. These nodal planes imply sign changes in the HOMO wave function and thus in the associated tunneling amplitude.

Strikingly, the nodal planes match with the locations where the Kondo and YSR spectra are symmetric and their asymmetries invert. This provides strong evidence for an interference model involving two molecular orbitals rather than parallel tunneling directly into the substrate (compare Ref. [22] for magnetic adatoms). For tip positions at the nodal planes, tunneling proceeds predominantly via the strongly exchange-coupled molecular orbital, and leads to symmetric Kondo and YSR line shapes. Because of the sign change in the amplitude for tunneling via the HOMO, the two tunneling paths interfere with opposite relative sign on the two sides of the nodal plane, explaining the observed inversion of the asymmetry in the Kondo line shape [see Fig. 4(a) for a sketch and SM [37] for a Green's-function calculation relating this sign change to the asymmetric Kondo line shape in Eq. (1)].

This model also provides a natural explanation for the YSR asymmetry and its correlations with the Kondo asymmetry. A shift of the YSR energy upon lifting the molecule further from the substrate using tip-molecule interactions implies that on the superconductor, the impurity spin is in the unscreened regime despite the sizable Kondo correlations [32,37]. Then, the ground state $|e\rangle$ of the superconducting substrate has even fermion parity and tunneling excites the substrate into the odd-parity state $|o\rangle = \gamma_\epsilon^\dagger |e\rangle$, in which the Bogoliubov quasiparticle (with annihilation operator γ_ϵ) associated with the YSR state is occupied. Because of the spin polarization of the YSR state [7–9,16,17,48–50], the odd-parity state $|o\rangle$ is only excited by electrons whose spin is antiparallel to the molecular spin, when tunneling from tip to substrate. Conversely, when tunneling from the substrate into the tip, the tunneling electron has parallel spin and leaves behind an excitation with antiparallel spin due to the spin-singlet nature of Cooper pairs [see Fig. 4(b) for a sketch]. This implies that the amplitude $\mp J_d$ for tunneling via the strongly exchange-coupled orbital has opposite signs for the two bias polarities, while the amplitude V_h for tunneling via the HOMO is spin independent. A Fermi's golden rule calculation gives (see SM [37] for details)

$$\left.\frac{dI}{dV}\right|_{\pm} \propto |\langle o|(\mp J_d S + V_h)\mathcal{O}_\pm|e\rangle|^2. \tag{2}$$

In accordance with our physical arguments, $\mathcal{O}_+ = \psi_\downarrow^\dagger$ at positive bias and $\mathcal{O}_- = \psi_\uparrow$ at negative bias, where ψ_σ annihilates a spin-σ electron in the substrate. For equal weights of the electron and hole YSR wave functions, we have $|\langle o|\psi_\downarrow^\dagger|e\rangle| = |\langle o|\psi_\uparrow|e\rangle|$, and the YSR asymmetry reflects that the two tunneling paths interfere with opposite

relative sign for the two bias polarities. The relative sign changes at the nodal plane due to V_h, explaining the asymmetry inversion of the YSR peaks and its correlation with the Kondo asymmetry. We note that the conclusions would remain qualitatively unchanged for a screened impurity spin. Our model also captures that the Kondo asymmetry as measured by the angle ϕ is small (compared to π), while the YSR asymmetry is large (of order unity) (for details, see SM [37]).

We find the lowest unoccupied molecular orbital (LUMO) at a significantly higher energy of 1.08 V, suppressing its contribution to the parallel channel. This is consistent with spatial maps of the LUMO [Fig. 3(c)], which have their highest intensity at the four pyridine legs and unlike the HOMO do not match the symmetry properties of the Kondo or YSR asymmetries.

In conclusion, we have shown that the asymmetry of the Kondo resonance across a magnetic molecule arises from interference between tunneling through different molecular orbitals, and need not involve direct tunneling into the substrate. Interference of the same tunneling paths also underlies a parallel asymmetry of the YSR resonances. Our observations also suggest an alternative understanding of YSR asymmetries, which have so far been typically interpreted in terms of different electron and hole wave functions due to potential scattering of substrate electrons on the magnetic impurity. While this interpretation suffices for magnetic adsorbates in the absence of additional tunneling paths [51,52], we expect that our model will be widely relevant for interpreting tunneling-spectroscopy experiments probing magnetic molecules on normal-metal and superconducting substrates.

We thank J. I. Pascual, C. Rubio-Verdú, and Rok Zitko for discussions and sharing their manuscript on a similar porphyrin molecule prior to submission [53]. We gratefully acknowledge funding by the European Research Council under the Consolidator Grant "NanoSpin," and by Deutsche Forschungsgemeinschaft through project C03 of CRC 183.

[1] V. Madhavan, W. Chen, T. Jamneala, M. F. Crommie, and N. S. Wingreen, Science **280**, 567 (1998).
[2] J. Li, W.-D. Schneider, R. Berndt, and B. Delley, Phys. Rev. Lett. **80**, 2893 (1998).
[3] A. Schiller and S. Hershfield, Phys. Rev. B **61**, 9036 (2000).
[4] O. Újsághy, J. Kroha, L. Szunyogh, and A. Zawadowski, Phys. Rev. Lett. **85**, 2557 (2000).
[5] M. Ternes, A. J. Heinrich, and W.-D. Schneider, J. Phys. Condens. Matter **21**, 053001 (2009).
[6] J. Figgins and D. K. Morr, Phys. Rev. Lett. **104**, 187202 (2010).
[7] L. Yu, Acta Phys. Sin. **21**, 75 (1965).
[8] H. Shiba, Prog. Theor. Phys. **40**, 435 (1968).
[9] A. I. Rusinov, JETP Lett. **9**, 85 (1969).
[10] T. Matsuura, Prog. Theor. Phys. **57**, 1823 (1977).
[11] O. Sakai, Y. Shimizu, H. Shiba, and K. Satori, J. Phys. Soc. Jpn. **62**, 3181 (1993).
[12] R. Zitko, J. S. Lim, R. López, and R. Aguado, Phys. Rev. B **91**, 045441 (2015).
[13] A. Yazdani, B. A. Jones, C. P. Lutz, M. F. Crommie, and D. M. Eigler, Science **275**, 1767 (1997).
[14] S.-H. Ji, T. Zhang, Y.-S. Fu, X. Chen, X.-C. Ma, J. Li, W.-H. Duan, J.-F. Jia, and Q.-K. Xue, Phys. Rev. Lett. **100**, 226801 (2008).
[15] K. J. Franke, G. Schulze, and J. I. Pascual, Science **332**, 940 (2011).
[16] M. E. Flatté and J. M. Byers, Phys. Rev. B **56**, 11213 (1997).
[17] M. I. Salkola, A. V. Balatsky, and J. R. Schrieffer, Phys. Rev. B **55**, 12648 (1997).
[18] A. V. Balatsky, I. Vekhter, and J. X. Zhu, Rev. Mod. Phys. **78**, 373 (2006).
[19] B. Liu, H. Fu, J. Guan, B. Shao, S. Meng, J. Guo, and W. Wang, ACS Nano **11**, 11402 (2017).
[20] C. Rubio-Verdú, A. Sarasola, D.-J. Choi, Z. Majzik, R. Ebeling, M. R. Calvo, M. M. Ugeda, A. Garcia-Lekue, D. Sánchez-Portal, and J. I. Pascual, Commun. Phys. **1**, 15 (2018).
[21] D. Rolf, C. Lotze, C. Czekelius, B. W. Heinrich, and K. J. Franke, J. Phys. Chem. Lett. **9**, 6563 (2018).
[22] S. Frank and D. Jacob, Phys. Rev. B **92**, 235127 (2015).
[23] J. Fernandez, P. Roura-Bas, and A. A. Aligia, arXiv: 2005.09090.
[24] U. G. E. Perera, H. J. Kulik, V. Iancu, L. G. G. V. Dias da Silva, S. E. Ulloa, N. Marzari, and S.-W. Hla, Phys. Rev. Lett. **105**, 106601 (2010).
[25] R. Requist, S. Modesti, P. P. Baruselli, A. Smogunov, M. Fabrizio, and E. Tosatti, Proc. Natl. Acad. Sci. U.S.A. **111**, 69 (2014).
[26] W. Wang, R. Pang, G. Kuang, X. Shi, X. Shang, P. N. Liu, and N. Lin, Phys. Rev. B **91**, 045440 (2015).
[27] J. Meyer, R. Ohmann, A. Nickel, C. Toher, R. Gresser, K. Leo, D. A. Ryndyk, F. Moresco, and G. Cuniberti, Phys. Rev. B **93**, 155118 (2016).
[28] Spatial variations of the bias asymmetry of Jahn-Teller excitations were observed in [29].
[29] J. Kügel, P.-J. Hsu, M. Böhme, K. Schneider, J. Senkpiel, D. Serrate, M. Bode, and N. Lorente, Phys. Rev. Lett. **121**, 226402 (2018).
[30] N. Hatter, B. W. Heinrich, M. Ruby, J. I. Pascual, and K. J. Franke, Nat. Commun. **6**, 8988 (2015).
[31] S. Kezilebieke, M. Dvorak, T. Ojanen, and P. Liljeroth, Nano Lett. **18**, 2311 (2018).
[32] L. Farinacci, G. Ahmadi, G. Reecht, M. Ruby, N. Bogdanoff, O. Peters, B. W. Heinrich, F. von Oppen, and K. J. Franke, Phys. Rev. Lett. **121**, 196803 (2018).
[33] L. Malavolti, M. Briganti, M. Hänze, G. Serrano, I. Cimatti, G. McMurtrie, E. Otero, P. Ohresser, F. Totti, M. Mannini, R. Sessoli, and S. Loth, Nano Lett. **18**, 7955 (2018).
[34] J. Brand, S. Gozdzik, N. Néel, J. L. Lado, J. Fernández-Rossier, and J. Kröger, Phys. Rev. B **97**, 195429 (2018).
[35] M. Etzkorn, M. Eltschka, B. Jäck, C. R. Ast, and K. Kern, arXiv:1807.00646.
[36] S. Kezilebieke, R. Zitko, M. Dvorak, T. Ojanen, and P. Liljeroth, Nano Lett. **19**, 4614 (2019).
[37] See Supplemental Material at http://link.aps.org/supplemental/10.1103/PhysRevLett.125.256805 for Experimental details;

additional data on (i) evolution of Kondo and YSR asymmetry along an FeTPyP molecule, (ii) magnetic field dependence of Kondo resonance, (iii) identification of YSR coupling regime; theoretical considerations including (i) model, (ii) Kondo resonance, (iii) YSR resonances; further comparison between theory and experiment.

[38] W. Auwärter, F. Klappenberger, A. Weber-Bargioni, A. Schiffrin, T. Strunskus, C. Wöll, Y. Pennec, A. Riemann, and J. V. Barth, J. Am. Chem. Soc. **129**, 11279 (2007).

[39] X. Chen, S. Lei, C. Lotze, C. Czekelius, B. Paulus, and K. J. Franke, J. Chem. Phys. **146**, 092316 (2017).

[40] B. W. Heinrich, L. Braun, J. I. Pascual, and K. J. Franke, Nano Lett. **15**, 4024 (2015).

[41] H. O. Frota and L. N. Oliveira, Phys. Rev. B **33**, 7871 (1986).

[42] H. O. Frota, Phys. Rev. B **45**, 1096 (1992).

[43] A. Rosch, T. A. Costi, J. Paaske, and P. Wölfle, Phys. Rev. B **68**, 014430 (2003).

[44] H. Prüser, M. Wenderoth, P. E. Dargel, A. Weismann, R. Peters, T. Pruschke, and R. G. Ulbrich, Nat. Phys. **7**, 203 (2011).

[45] M. Gruber, A. Weismann, and R. Berndt, J. Phys. Condens. Matter **30**, 424001 (2018).

[46] M. Ruby, B. W. Heinrich, J. I. Pascual, and K. J. Franke, Phys. Rev. Lett. **114**, 157001 (2015).

[47] E. Minamitani, Y.-S. Fu, Q.-K. Xue, Y. Kim, and S. Watanabe, Phys. Rev. B **92**, 075144 (2015).

[48] V. Kaladzhyan, C. Bena, and P. Simon, Phys. Rev. B **93**, 214514 (2016).

[49] S. Körber, B. Trauzettel, and O. Kashuba, Phys. Rev. B **97**, 184503 (2018).

[50] L. Cornils, A. Kamlapure, L. Zhou, S. Pradhan, A. A. Khajetoorians, J. Fransson, J. Wiebe, and R. Wiesendanger, Phys. Rev. Lett. **119**, 197002 (2017).

[51] M. Ruby, Y. Peng, F. von Oppen, B. W. Heinrich, and K. J. Franke, Phys. Rev. Lett. **117**, 186801 (2016).

[52] D.-J. Choi, C. Rubio-Verdú, J. De Bruijckere, M. M. Ugeda, N. Lorente, and J. I. Pascual, Nat. Commun. **8**, 15175 (2017).

[53] C. Rubio-Verdú, J. Zaldivar, R. Zitko, and J. I. Pascual, arXiv:2007.12091.